

## GCMS, FTIR, SEM, Physiochemical and Rheological Studies on *Albizia zygia* Gum

Nnabuk Okon EDDY<sup>1</sup>, Stephen Eyije ABECHI<sup>1,\*</sup>, Paul AMEH<sup>1</sup> and Eno E. EBENSO<sup>2</sup>

<sup>1</sup>Department of Chemistry, Ahmadu Bello University, Zaria, Kaduna State, Nigeria

<sup>2</sup>Department of Chemistry, School of Mathematical & Physical Sciences, North-West University, Mafikeng Campus, Mmabatho 2735, South Africa

(\*Corresponding author's e-mail: abeshus@yahoo.com, nabukeddy@yahoo.com)

Received: 3 March 2012, Revised: 24 May 2012, Accepted: 31 March 2013

### Abstract

GCMS (Gas Chromatography Mass Spectrometry), FTIR (Fourier Transformed Infra-Red Spectroscopy), SEM (Scanning Electron Microscopy), physiochemical and rheological analysis of *Albizia zygia* gum have been carried out. *Albizia zygia* exudate is a brownish in colour, acidic and ionic gum. GCMS spectra of the gum indicated the presence of (*E*)-methyl octadec-7-enoate (41.18 %), methyl palmitate (18.64 %), methyl stearate (19.13 %), (9*E*,12*E*)-methyl octadeca-9,12-dienoate (11.88 %), methyl icosanoate (1.85 %), 2,3-dihydroxypropyl oleate (2.05 %), (*Z*)-octadec-13-enal (1.63 %), 2-hydroxy-3-(palmitoyloxy)propyl stearate (1.55 %), 2,3-dihydroxypropyl stearate (0.82 %), dimethyl phthalate (0.58 %) and 3-((aminomethoxy) (hydroxy)phosphoryloxy)propane-1,2-diyl dipalmitate (0.70 %). The FTIR spectrum of the gum indicated several functional groups, including –OH, C–O and C=O. From the scanning electron micrograph, the morphology of the gum shows irregular shapes embedded on the surface. Rheological studies indicated that the viscosity of the gum increased with increasing pH but decreased with an increase in temperature. Application of Huggins, Kraemer and Tanglertpaibul and Rao models indicated that the intrinsic viscosity of the gum is in the range of 0.5 - 0.8. Plots obtained for the variation of viscosity with shear rate and shear rate with shear stress confirmed that *Albizia zygia* gum is a non Newtonian dilatant polymer with a characteristic shear thickening property.

**Keywords:** *Albizia zygia* gum, physiochemical studies of gum, rheological analysis, Huggins model, Kraemer model, Tanglertpaibul and Rao model

### Introduction

*Albizia* gum is derived from trees of the genus *Albizia* and is formed as round elongated bars of variable size and colour ranging from yellow to dark brown [1]. Results obtained from elemental analysis indicated that gum exudates derived from the genus *Albizia* are complex salts of calcium, potassium, magnesium and sodium, in decreasing proportions. Other metals like zinc, copper, iron, lead and aluminum are present in trace amounts [2]. *Albizia* gum is soluble in water, forming a colourless mucilage with a bland taste.

Plant gums have been found to be useful in the pharmaceutical, food and other industries [2]. Some are used as adhesives and others as food additives. However, utilization of a given plant gum depends on its physiochemical and rheological parameters. Due to their broad spectrum of applications, some plant gums have been studied. For example, Mhinzi [3] studied physiochemical properties of selected *Albizia* species from Tanzania and found that they have some common physiochemical properties. de Paul *et al.* [2] investigated the chemical and rheological

properties of *Albizia lebbeks* gum using  $^{13}\text{C}$  NMR spectroscopy and Ubbelohde viscometer and found that the gum is a low viscous polysaccharide with an apparent flow activation energy of 16.6 and 17.2 kJ/mol. Distribution of molecular components in *Acacia Senegal* gum has been studied by Siddig *et al.* [4] and it was deduced that the 3 main components of the gum are arabinogalactan protein, arabinogalactan and glycoprotein. Jalali *et al.* [5] studied the chemical composition of oleo-gum-resin from *Ferula gummosa* and found that the resin consists of various constituents including terpenes and alkaloids. Rheological properties of xanthan and locust bean gum have been studied by Higiroy *et al.* [6]; the gums were found to obey Huggins and power law models and from the rheological modeling of the gums, the conformation of the gums was established.

Also, several chemical instrumentations have been reportedly used for studying gums. The major ones include GCMS, FTIR, SEM, nuclear magnetic resonance spectroscopy (NMR), and differential scanning spectroscopy (DSC). Bonaduce *et al.* [7] used GCMS to characterize plant gums in samples from painted work of art. Dutta and Sarkar [8] used Infrared absorption spectrum to study the change in characteristics bond and the vibration of biomolecules in gum Arabic. Shifts in characteristics frequency were attributed to changes in the molecular structure of the gum due to polymerization effects. Zhang *et al.* [9] characterized tamarind gum/sodium alginate composite gel beads using a differential scanning calorimeter. The obtained FTIR and SEM information was significant. Monteiro *et al.* [10] used SEM to study the morphology of polymers on hair fibre and found that the polymers accumulate in the hair fibre and continuously improved the hair.

In spite of the broad spectrum of researches carried out on plant gums, literature on detailed chemical and rheological properties of *Albizia zygia* gum (especially those of Nigerian origin) is rare. Literature on the application of FTIR, GCMS and SEM instrumentations are also scanty. Therefore, the aim of the present study is to study the physiochemical and rheological properties of *Albizia zygia* gum using FTIR, SEM, GCMS and viscometer instrumentations.

## Materials and methods

### Collection of samples

Crude *Albizia zygia* gum was obtained as dried exudates from their parent trees grown in the Falgore forest in Doguwa Local Government Area of Kano State, Nigeria.

### Purification of the gum

The procedure adapted for the purification of the gum was that of Femi-Oyewo *et al.* [11]. A crude sample of *Albizia zygia* gum was dried in an oven at 40 °C for 2 h, and its size was reduced using a blender. The sample was further hydrated in double strength chloroform water for 5 days with intermittent stirring to ensure complete dissolution of the gum, and then strained through a 75  $\mu\text{m}$  sieve to obtain particle-free slurry which was allowed to sediment. Thereafter, the gum was precipitated from the slurry using absolute ethanol, filtered and defatted with diethyl ether. The precipitate was redried at 40 °C for 48 h. The dried flakes were pulverized using a blender and stored in an air tight container.

### Physiochemical analysis

#### Determination of percentage yield of the purified gums

The dried, precipitated and purified gum(s) obtained from the crude dried exudates were weighed and the percentage yields were expressed in percentage, using the weight of the crude gum(s) as the denominator.

#### Determination of solubility in various solvents

The solubility of the gum was determined in cold and hot distilled water, acetone, chloroform and ethanol. One g sample of the gum was added to 50 ml of each of the above mentioned solvents and left overnight. Twenty five ml of the clear supernatants was placed in small pre-weighted evaporating dishes and heated to dryness over a digital thermostatic water bath. The weights of the residue with reference to the volume of the solutions were determined using a digital top loading balance (Model XP-3000) and expressed as the percentage solubility of the gums in the solvents [12].

#### Determination of pH

This was done by shaking a 1 % w/v dispersion of the sample in water for 5 min and the pH was determined using a pre-calibrated Oaklon pH meter (Model 1100).

#### Viscosity measurements

The intrinsic viscosity of the gum samples was determined in distilled water using a Cannon Ubbelohde capillary viscometer (Cannon Instruments, model I-71) which was immersed in a water bath at a temperature of 25 °C. The apparent viscosity of the mucilage was measured using a digital Brookfield DV I prime viscometer.

#### FTIR analysis

FTIR analyses of the gums were carried out using a Scimadzu FTIR-8400S Fourier Transform Infra-red Spectrophotometer. The sample was prepared using KBr and the analysis was done by scanning the sample through a wave number range of 400 to 4,000  $\text{cm}^{-1}$ .

#### GC-MS analysis

The analysis was carried out on a GC clarus 500 Perkin Elmer system comprising of a AOC-20i Autosampler and Gas Chromatograph interfaced to a Mass Spectrometer (GC-MS). The instrument employed the following conditions: a column Elite-1 fused silica capillary column ( $30 \times 0.25 \text{ mm ID} \times 1 \mu\text{m df}$ , composed of 100 % Dimethyl poly dioxane), operating in electron impact mode at 70 eV. Helium (99.999 %) was used as carrier gas at a constant flow of 1 ml/min and an injection volume of 0.5  $\mu\text{L}$  was employed (split ratio of 10:1) with an injector temperature of 250 °C; an ion-source temperature of 280 °C. The oven temperature was programmed from 110 °C (isothermal for 2 min), with an increase of 10 °C/min, to 200 °C, then 5 °C/min to 280 °C, ending with a 9 min isothermal at 280 °C. Mass spectra were taken at 70 eV; a scan interval of 0.5 seconds and fragments from 40 to 450 Da. The total GC running time was 36 min.

#### Interpretation of GC-MS spectrum

Interpretation of the mass spectrum GC-MS was conducted using the database of National Institute Standard and Technology (NIST), which has more than 62,000 patterns. The spectrum of the unknown component was compared with the spectrum of the known components stored in the NIST library. The name, molecular weight and structure of the components of the test materials were ascertained. Concentrations of the identified compounds were determined through area and height normalization.

#### Scanning electron microscopy

The morphological features of the gums were studied with a JSM-5600 LV Scanning Electron Microscope (SEM) from JEOL, Tokyo, Japan. The dried sample was mounted on a metal stub and sputtered with gold in order to make the sample conductive, and the images were taken at an accelerating voltage of 10 kV.

### Results and discussions

#### Physiochemical parameters of *Albizia zygia* gum

**Table 1** presents physiochemical parameters of *Albizia zygia* gum. From **Table 1**, it can be seen that the colour of a crude sample of *Albizia zygia* gum is dark brown (**Figure 1**). The gum has a honey odour and its taste is bland. The measured pH of the gum was 4.7, indicating that the gum is mild acidic. After purification, the gum yield was 56 %. *Albizia zygia* gum is insoluble in common organic solvents like acetone and chloroform but sparingly soluble in ethanol (about 0.04 % w/v). However, the gum is soluble in hot and cold water. Its solubility in water decreases with an increase in temperature. From a solubility point of view, *Albizia zygia* gum is ionic, because it dissolves in water, which has a high dielectric constant, and partly in ethanol, whose dielectric constant is higher than that of acetone and chloroform.

**Table 1** Physiochemical parameters of *Albizia zygia* gum.

| Parameters               | <i>Albizia zygia</i> gum |
|--------------------------|--------------------------|
| Colour                   | Dark – Brown             |
| Odour                    | Honey                    |
| Taste                    | Bland                    |
| pH                       | 4.7                      |
| Percentage yield (% w/w) | 56 %                     |
| Solubility (% w/v)       |                          |
| Cold water               | 13.4 %                   |
| Hot water                | 15.6 %                   |
| Acetone                  | 0.0 %                    |
| Chloroform               | 0.0 %                    |
| Ethanol                  | 0.4 %                    |



**Figure 1** Crude samples of *Albizia zygia* gum.

#### GC-MS study

**Figure 2** shows the GC-MS spectrum of *Albizia zygia* gum. From this Figure, it is evident that the spectrum of *Albizia zygia* gum consists of eleven peaks. In **Figure 3**, chemical structures of compounds likely identified from a spectral library are presented. Since the area under a chromatogram is proportional to the concentration of the active species, values of area under the chromatogram for each peak (obtained from area normalization), associated concentrations, fragmentation peaks (obtained from mass spectra), base and mass peaks are presented in **Table 2**.

The first 5 peaks of the GCMS spectrum of *Albizia zygia* gum indicate the presence of various substituted esters, namely, dimethyl phthalate (line 1), methyl palmitate (line 2), (9*E*,12*E*)-methyl octadeca-9,12-dienoate (line 3), (*E*)-methyl octadec-7-enoate (line 4) and methyl stearate (line 5). The chemical structures of these compounds are numbered (**Figure 3**) using the line number in which they appear in the spectrum. These compounds were found to constitute the most abundant components of the *Albizia zygia* gum and the measured concentrations were 0.58, 18.64, 11.88, 41.18 and 19.13 % respectively. The

retention times for the separated compounds were 9.817, 15.367, 16.942, 17.058 and 17.283 min respectively. The mass and various fragmentation peaks identified for the separated compounds are recorded in **Table 2**.

Lines 6 to 11 indicates the presence of various substituted carboxylic acids aldehyde

namely 3-(aminomethoxy) (hydroxy)phosphoryloxy)propane-1,2-diyl dipalmitate (the sixth peak), methyl icosanoate (the seventh peak), (*Z*)-octadec-13-enal (line 8), 2-hydroxy-3-(palmitoyloxy)propyl stearate (the ninth peak), 2,3-dihydroxypropyl oleate (line 10) and 2,3-dihydroxypropyl stearate (the eleventh peak).

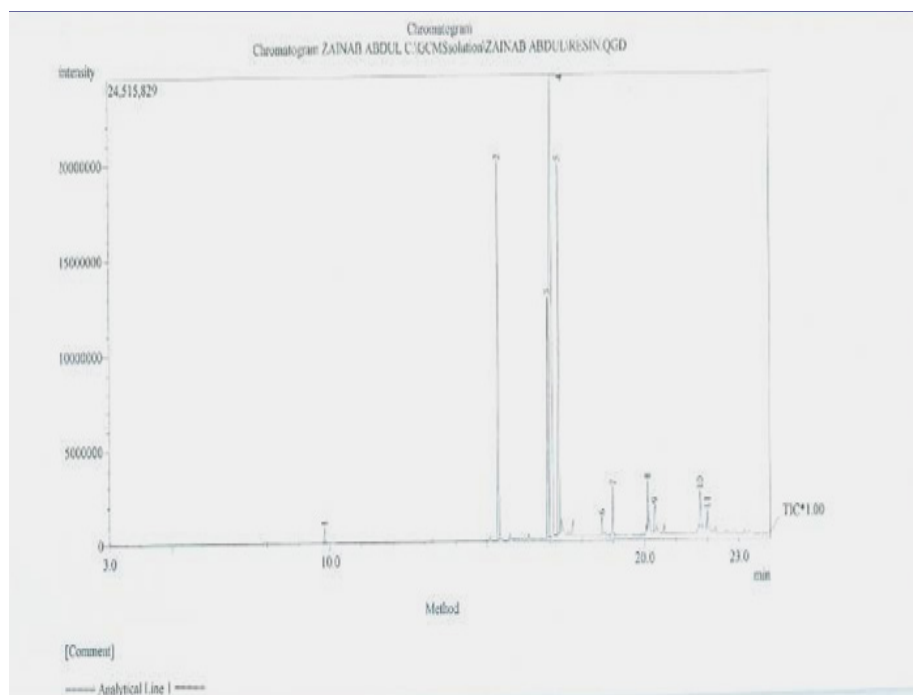


**Figure 2** GC-MS spectrum of *Albizia zygia* gum.

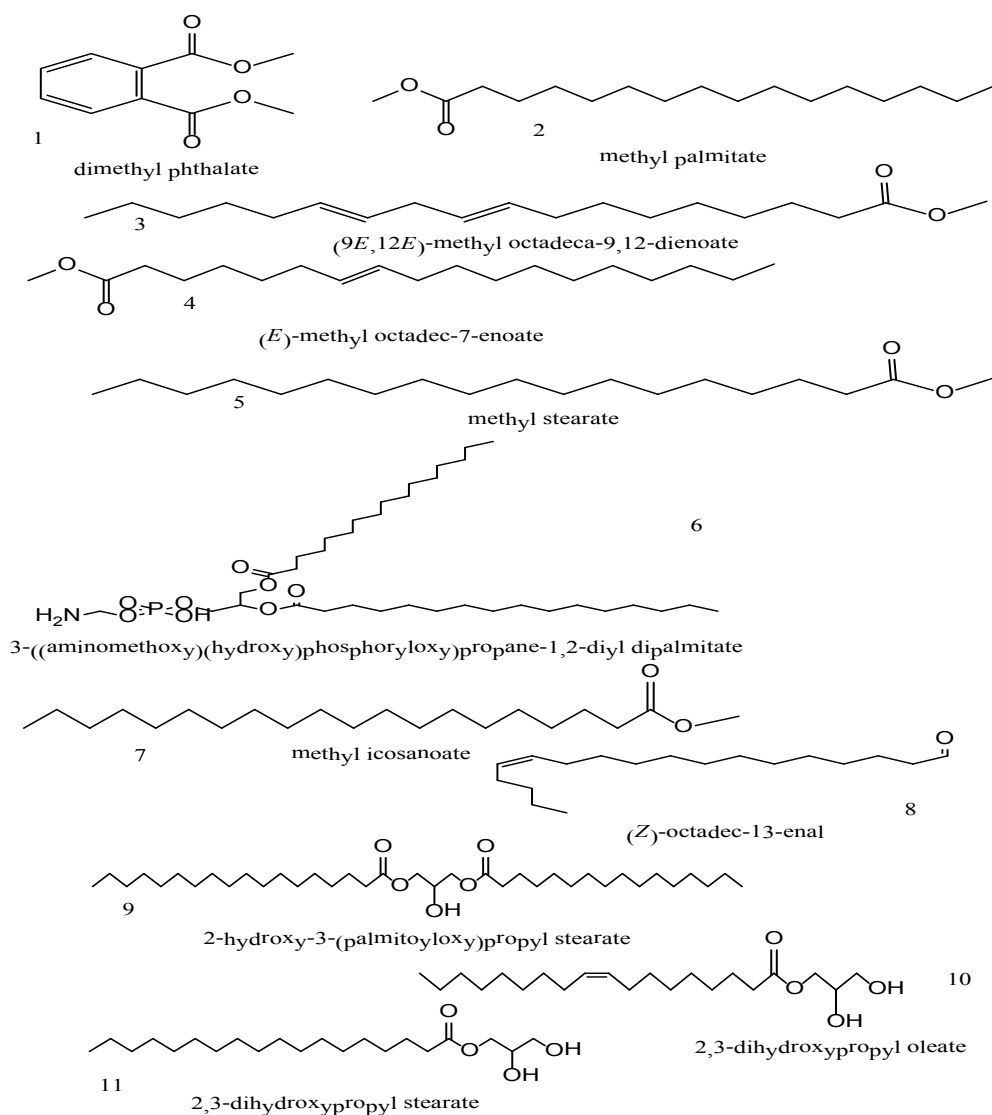


**Figure 3** Chemical structures of compounds identified in the GC-MS spectrum of *Albizia zygia*.

**Table 2** Characteristics of compounds identified from GC-MS of *Albizia zygia* gum.

| Line No | IUPAC Name  | Molecular formula                                 | Molar mass (g/mol) | RT(m)  | Mass peak (amu) | % Conc. | Fragmentation peak  |
|---------|---|---|--------------------|--------|-----------------|---------|---|
| 1       | dimethyl phthalate  | C <sub>10</sub> H <sub>10</sub> O <sub>4</sub>    | 194                | 9.817  | 42              | 0.58    | 30(2%), 39(5%), 50(35%), 64(10%), 77(80%), 92(30%), 104(15%), 120(5%), , 133(15%), 163(100%), 194(15%).   |
| 2       | methyl palmitate  | C <sub>17</sub> H <sub>34</sub> O <sub>2</sub>    | 270                | 15.367 | 132             | 18.64   | 30(2%), 41(20%), 57(20%), 74(100%), 87(70%), 101(10%), 115(2%), 129(5%), 143(10%), 157(2%), 171(5%), 185(5%), 199(5%), 213(2%), 227(10%), 239(5%), 270(10%).  |
| 3       | (9E,12E)-methyl octadeca-9,12-dienoate                                | C <sub>19</sub> H <sub>34</sub> O <sub>2</sub>    | 294                | 16.942 | 165             | 11.88   | 30(2%), 41(55%), 55(75%), 67(100%), 81(90%), 95(60%), 109(25%), 123(10%), 135(5%), 150(5%), 164(5%), 178(5%), 192(2%), 205(2%), 222(2%), 234(2%), 245(2%), 265(10%), 294(10%).                                |
| 4       | (E)-methyl octadec-7-enoate   | C <sub>19</sub> H <sub>36</sub> O <sub>2</sub>    | 296                | 17.058 | 191             | 41.18   | 30(2%), 41(55%), 55(100%), 69(75%), 83(70%), 97(65%), 123(15%), 137(10%), 152(5%), 166(5%), 180(15%), 194(2%), 207(2%), 222(20%), 235(5%), 246(5%), 264(30%), 266(15%), 296 (10%).                            |
| 5       | methyl stearate   | C <sub>19</sub> H <sub>38</sub> O <sub>2</sub>    | 298                | 17.283 | 145             | 19.13   | 30(2%), 41(20%), 43(35%), 57(20%), 74(100%), 87(75%), 101(10%), 115(2%), 129(5%), 143(10%), 157(2%), 171(2%), 185(5%), 199(10%), 213(5%), 227(2%), 241(5%), 255(10%), 267(5%), 298 (15%).                     |
| 6       | 3-((aminomethoxy) (hydroxy)phosphoryloxy)propane-1,2-diyl dipalmitate | C <sub>17</sub> H <sub>74</sub> NO <sub>8</sub> P | 691                | 18.658 | 69              | 0.70    | 31(15%), 41(55%), 43(80%), 57(100%), 83(30%), 84(40%), 98(75%), 116(50%), 129(30%), 171(5%), 185(5%), 213(5%), 227(5%), 239(15%), 269(10%), 283(5%).  |
| 7       | methyl icosanoate   | C <sub>21</sub> H <sub>42</sub> O <sub>2</sub>    | 326                | 19.008 | 91              | 1.85    | 31(2%), 41(30%), 43(51%), 57(30%), 74(100%), 87(70%), 101(5%), 115(2%), 129(2%), 143(5%), 157(2%), 171(2%), 185(2%), 199(2%), 213(2%), 227(2%), 241(2%), 255(2%), 269(2%), 283 (2%), 295(2%), 326(5%).        |
| 8       | (Z)-octadec-13-enal   | C <sub>18</sub> H <sub>34</sub> O                 | 266                | 20.108 | 129             | 1.63    | 30(15%), 41(70%), 55(100%), 57(60%), 81(50%), 95(40%), 116(10%), 129(50%), 152(5%), 165(5%), 185(10%), 199(2%), 221(5%), 235(5%), 265(5%), 281 (2%), 295(5%), 309(2%).  |
| 9       | 2-hydroxy-3-(palmitoyloxy)propyl stearate                             | C <sub>39</sub> H <sub>76</sub> O <sub>5</sub>    | 624                | 20.325 | 81              | 1.55    | 30(15%), 41(40%), 43(75%), 57(100%), 83(40%), 98(60%), 116(65%), 129(50%), 143(5%), 154(2%), 171(10%), 185(15%), 199(5%), 213(5%), 227(5%), 241(5%), 255(5%), 267(10%), 283 (5%), 283(5%), 297(15%), 311(5%). |
| 10      | 2,3-dihydroxypropyl oleate  | C <sub>21</sub> H <sub>40</sub> O <sub>4</sub>    | 356                | 21.758 | 116             | 2.05    | 30(10%), 41(60%), 55(100%), 69(55%), 81(55%), 95(40%), 98(70%), 112(40%), 137(10%), 151(5%), 166(5%), 180(5%), 207(5%), 221(10%), 235(10%), 247(5%), 264(40%), 266(30%), 251 (2%), 307(2%), 325(2%).          |
| 11      | 2,3-dihydroxypropyl stearate  | C <sub>21</sub> H <sub>42</sub> O <sub>4</sub>    | 358                | 21.983 | 86              | 0.82    | 31(10%), 41(60%), 43(100%), 57(90%), 74(60%), 84(55%), 98(95%), 112(40%), 134(40%), 147(10%), 154(10%), 185(5%), 199(5%), 210(10%), 241(5%), 264(5%), 267(40%), 285 (15%), 298(10%), 327(15%).                |

The concentrations of these compounds (**Table 2**) were low and ranged from 0.82 % (in line 11; 2, 3-dihydroxypropyl stearate) to 1.85 % (in line 7; methyl icosanoate). The retention time (**Table 2**) for compounds within this group extended from 18.658 to 21.983 min. In **Table 2**, base peaks, mass peaks and fragmentation peaks are presented.

It can be seen from the data that each of the identified compounds have characteristic numbers and nature of peaks. From the analysed chemical constituents of the studied gum, it is indicative that this gum is not poisonous and can therefore be used in food and pharmaceutical industries as reported elsewhere [3].

#### FTIR study

**Figure 4** shows the FTIR spectrum of *Albizia zygia* gum. Wave numbers and intensities

of adsorption peaks deduced from the spectrum, as well as the assignment of vibration type and functional group, are presented in **Table 3**. From the results obtained, it can be seen that the FTIR spectrum of the gum consists of several C-H bending which occurred in the wave number range of 703.08 to 1003.98 cm<sup>-1</sup>, C-O stretching (1084.03 - 1243.16 cm<sup>-1</sup>), C-N stretching (1321.28 cm<sup>-1</sup>), N-H bending (1594.22 and 1615.44 cm<sup>-1</sup>), C-H scissoring and bending (1423.51 and 1479.45 cm<sup>-1</sup>). Other vibrations included C=C stretching at 1662.69 cm<sup>-1</sup>, C≡C stretching at 2137.20 cm<sup>-1</sup>, O-H stretching at 2785.30, 2785.30, 3125.75 and 3251.13 cm<sup>-1</sup>. C-H bending at 1735.03 cm<sup>-1</sup>, C-H stretching at 2914.54, 3026.41 and 3483.56 cm<sup>-1</sup> as well as N- H stretching at 3368.79 cm<sup>-1</sup>.

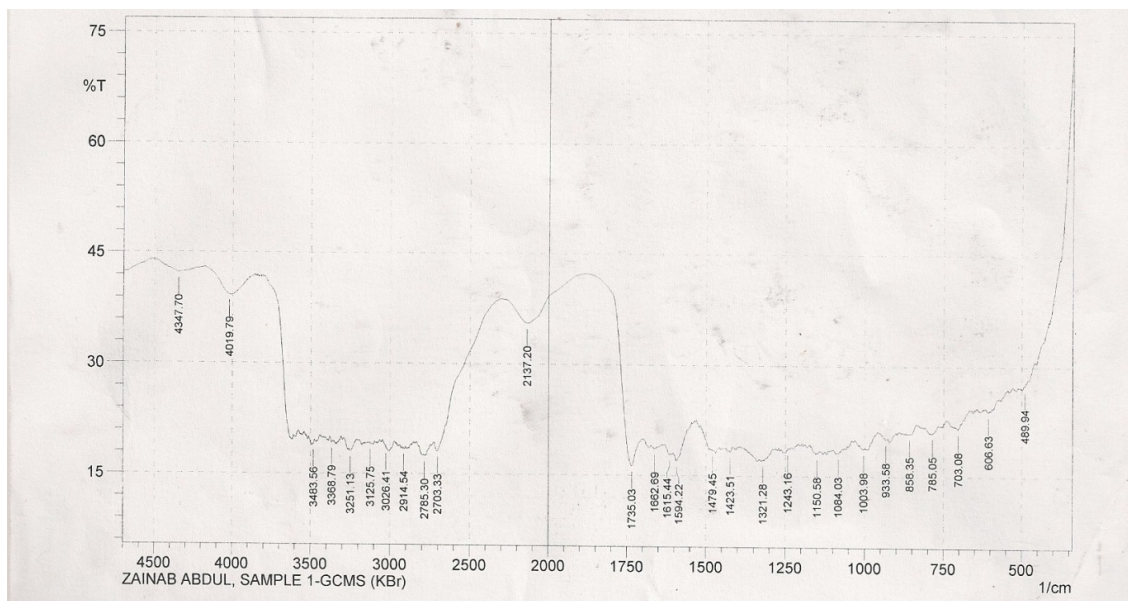


**Figure 4** FTIR spectrum of *Albizia zygia* gum.

**Table 3** Peaks and intensity of adsorption of FTIR by *Albizia zygia* gum.

| Peak (cm <sup>-1</sup> ) | Intensity | Assignment (functional group)                          |
|--------------------------|-----------|--|
| 703.08                   | 21.507    | C-H bending, phenyl ring substitution band             |
| 785.05                   | 20.887    | C-H bending, phenyl ring substitution band             |
| 858.35                   | 20.822    | C-H bending, phenyl ring substitution band             |
| 933.58                   | 20.021    | C-H bending, alkene                                    |
| 1003.98                  | 18.675    | C-H bending, alkene                                    |
| 1084.03                  | 18.115    | C-O stretching, carboxylic acid, ether, ester, alcohol |
| 1150.58                  | 18.043    | C-O stretching, carboxylic acid, ether, ester, alcohol |
| 1243.16                  | 18.610    | C-O stretching, carboxylic acid, ether, ester, alcohol |
| 1321.28                  | 17.092    | C-N stretching, amine                                  |
| 1423.51                  | 18.245    | C-H scissoring and bending, alkanes                    |
| 1479.45                  | 18.467    | C-H scissoring and bending, alkanes                    |
| 1594.22                  | 16.990    | C=C aromatic stretching                                |
| 1615.44                  | 17.772    | N-H bending, amines                                    |
| 1662.69                  | 18.586    | C=C stretching, alkene                                 |
| 1735.03                  | 16.277    | C-H bending, phenyl ring substitution overtone         |
| 2137.20                  | 35.556    | C≡C stretching, alkyne                                 |
| 2703.33                  | 18.065    | O-H stretching, carboxylic acid                        |
| 2785.30                  | 17.436    | O-H stretching, carboxylic acid                        |
| 2914.54                  | 18.425    | C-H stretching   |
| 3026.41                  | 18.501    | C-H stretching, alkene                                 |
| 3125.75                  | 19.035    | O-H stretching   |
| 3251.13                  | 18.023    | O-H stretching, alcohol, phenol                        |
| 3368.79                  | 19.172    | N-H stretching, amine                                  |
| 3483.56                  | 18.942    | C-H stretching   |

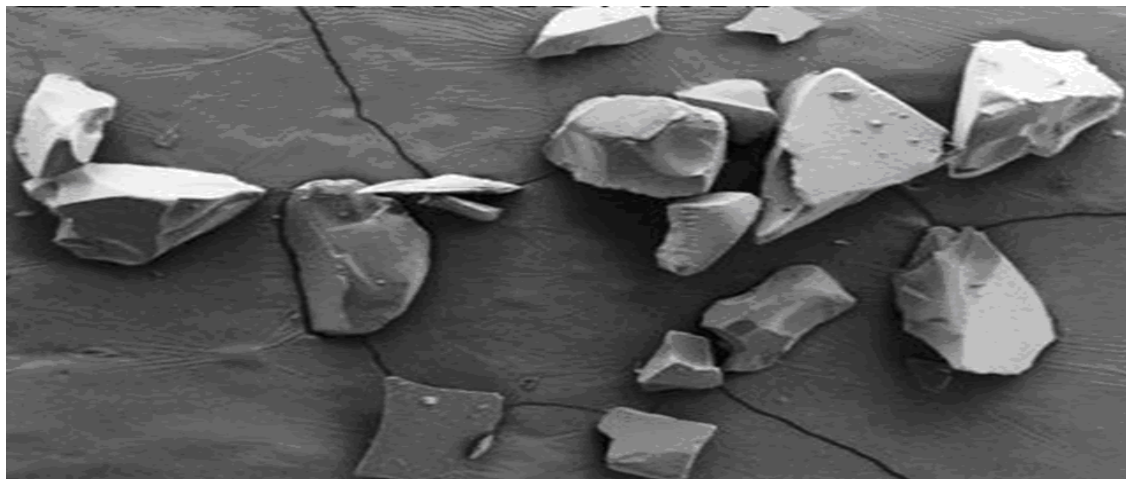


**Figure 5** Scanning electron micrograph of *Albizia zygia*.

#### Scanning electron microscopy (SEM)

**Figure 5** shows the scanning electron micrograph of *Albizia zygia* gum taken at an accelerating voltage of 10 kV and at 1000 $\times$  magnification and 50  $\mu$ m scale. From the Figure, it can be seen that the morphology of the gum is irregular in shape.

#### Rheological study

**Figure 6** shows variation of the viscosity of *Albizia zygia* gum with pH. From the **Figure 6**, it can be seen that the viscosity of the gum increases with increasing pH (to pH of 6). After this critical pH, the viscosity of the gum was unaffected by further change in pH indicating that the emulsifying properties of the gum is pH dependent and that the gum is ionic [13,14]. Viscosity of a liquid is related to the ease with which the molecules can move with respect to one another. Thus the viscosity of a liquid depends on the strength of attractive forces between molecules, which depend on their composition, size, and

shape, and also on the kinetic energy of the molecules, which depends on the temperature. This also implies that the strength of hydrogen bonding between the molecules of the gums can partly be a factor in accounting for the increase in viscosity with pH. At higher pH (that is, increasing alkalinity), the viscosity of the gum is expected to increase.

**Figure 7** shows variation of viscosity of *Albizia zygia* gum with temperature. Values of viscosity were recorded between the temperature ranges of 30 to 40  $^{\circ}$ C, and in order to verify the onset of degradation or conformational transitions during heating, the viscosity of the gums were again measured as cooling proceeded. The tests did not indicate any difference between the 2 set of data, suggesting that there was no degradation or conformational transition upon heating the gum [2].

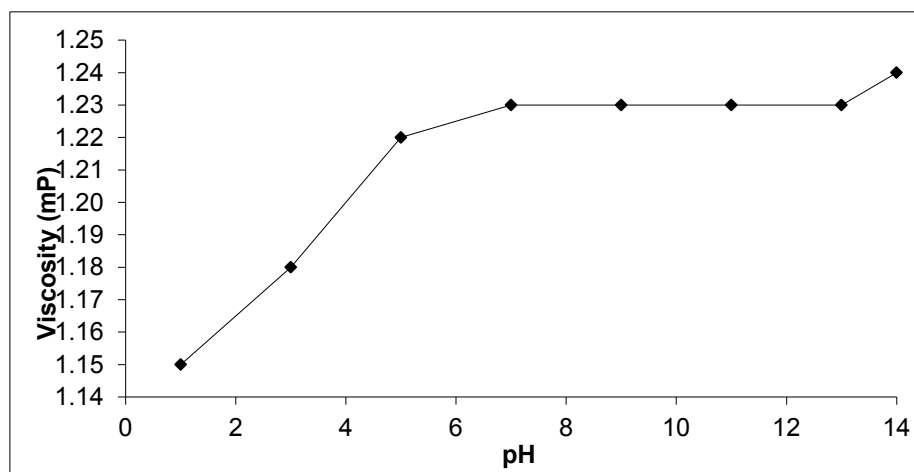


**Figure 6** Variation of viscosity of *Albizia zygia* gum with pH.

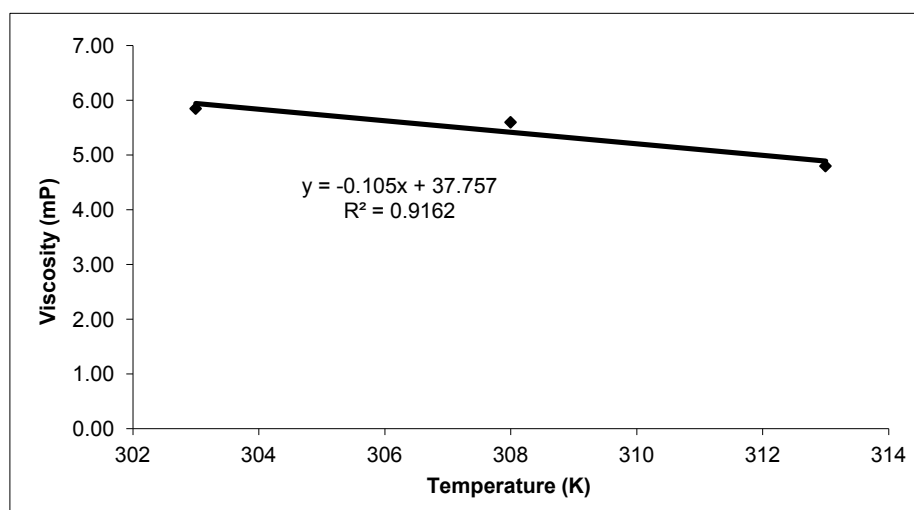


**Figure 7** Variation of viscosity of *Albizia zygia* gum with temperature.

**Figure 7** also revealed that the viscosity of the gums decreased with increasing temperature. This may be attributed to increasing breakage of intermolecular bonds between adjacent layers due to increasing kinetic motion at higher temperatures. The temperature dependence of viscosity is the phenomenon by which viscosity tends to decrease (or, alternatively, its fluidity tends to increase) as its temperature increases. Several models have been proposed to explain the dependence of viscosity on temperature. The exponential model states that the viscosity of a system varies exponentially with temperature, according to the following Eq. (1),

$$\eta = \eta_0 \exp(-bT) \quad (1)$$

where  $T$  is temperature and  $\eta_0$  and  $b$  are coefficients. Taking logarithm of both sides of Eq. (1) yields Eq. (2) below [2].

$$\ln(\eta) = \ln\eta_0 - bT \quad (2)$$

By plotting values of  $\log(\eta)$  versus  $T$  (plot not shown), a straight line ( $R^2 = 0.9162$ ) was obtained. Calculated values of  $\log(\eta_0)$  and  $b$  were  $-0.105$  and  $37.757$  respectively.

The Arrhenius model is another model that can be used to study the relationship between viscosity and temperature. This model is based on the assumption that fluid flow obeys the Arrhenius equation for molecular kinetics and can be written as follows,

$$\eta = \eta_0 \exp(E_a/RT) \quad (3)$$

where  $T$  is temperature,  $\eta_0$  is the Arrhenius coefficient,  $E_a$  is the activation energy and  $R$  is the universal gas constant. A first-order fluid is another name for a power law fluid with exponential dependence of viscosity on temperature. From the logarithm of Eq. (3), a plot of  $\ln(\eta)$  versus  $1/T$  should be a straight line with intercept and slope equal to  $\ln(\eta_0)$  and  $E_a/2.303R$  respectively. The results obtained indicated a linear ( $R^2 = 0.9003$ ) relationship between  $\ln(\eta)$  and  $1/T$ . From the slope and intercept of the plot (plot not shown), calculated values of  $E_a$  and  $\eta_0$  were  $15.52$  kJ/mol and  $0.1487$  respectively. The calculated value of the apparent activation energy of flow is very low, indicating the existence of few

inter and intra-interactions between the molecules of the gum.

Several important viscosity functions are used in viscosity studies. The intrinsic viscosity,  $[\eta]$  is a measure of the inherent ability of a polymer to increase solution viscosity. It is a measure of the hydrodynamic volume occupied by a macromolecule, which is closely related to the size and conformation of the macromolecular chains in a particular solvent [6,15]. The relative viscosity,  $\eta_{rel} = \eta_{solution}/\eta_{solvent}$ , is the dimensionless ratio of solution viscosity to solvent viscosity. The specific viscosity is the difference between relative viscosity and unity (i.e.,  $\eta_{spec} = (\eta_{rel} - 1)$ ) and is related to the fluid viscosity increase due to all polymer solute molecules. The reduced viscosity,  $\eta_{red} = \eta_{spec}/C$  is the fluid viscosity increase per unit of polymer solute concentration,  $C$ .

The intrinsic viscosity,  $[\eta]$  is the limit of the reduced viscosity as the polymer solute concentration approaches zero (Eq. 4)

$$[\eta] = \lim_{C \rightarrow 0} \frac{\eta_{spec}}{C} \quad (4)$$

The intrinsic viscosity of a polymer can be determined experimentally using Eq. (5), which is a power series in concentration,

$$\eta_{spec}/C = [\eta] + k_1[\eta]^2C + k_2[\eta]^3C^2 + k_3[\eta]^4C^3 \quad (5)$$

where  $[\eta]$  is the intrinsic viscosity and  $\eta_{spec}$  is the specific viscosity.  $k_1, k_2, k_3, \dots$  are dimensionless constants. Since  $\eta_{spec}/C$  is the reduced viscosity, and as  $C \rightarrow 0$ , it becomes the intrinsic viscosity. Hence, the above power series equation is often truncated to a linear approximation known as the Huggins equation [16]

$$\eta_{red} = [\eta] + k'[\eta]^2C \quad (6)$$

where  $[\eta]$  is the intrinsic viscosity and  $k'$  is the Huggins constant. From Eq. (5), a plot of  $\eta_{red}$  versus  $C$  is expected to be linear with intercept and slope equal to  $[\eta]$  and  $k'[\eta]^2$  respectively. **Figure 8** shows Huggins plot for *Albizia zygia* gum. Values of Huggins parameters deduced from the plots are presented in **Table 4**.

**Table 4** Huggins and Kraemer parameters for *Albizia zygia* gum.

|         | Slope  | $[\eta]$ | $[\eta]^2$ | K      | $R^2$  |
|---------|--------|----------|------------|--------|--------|
| Huggins | 1.0188 | 0.7604   | 0.5047     | 1.4341 | 0.8150 |
| Kraemer | 0.8325 | 0.8145   | 0.6634     | 1.0221 | 0.9039 |

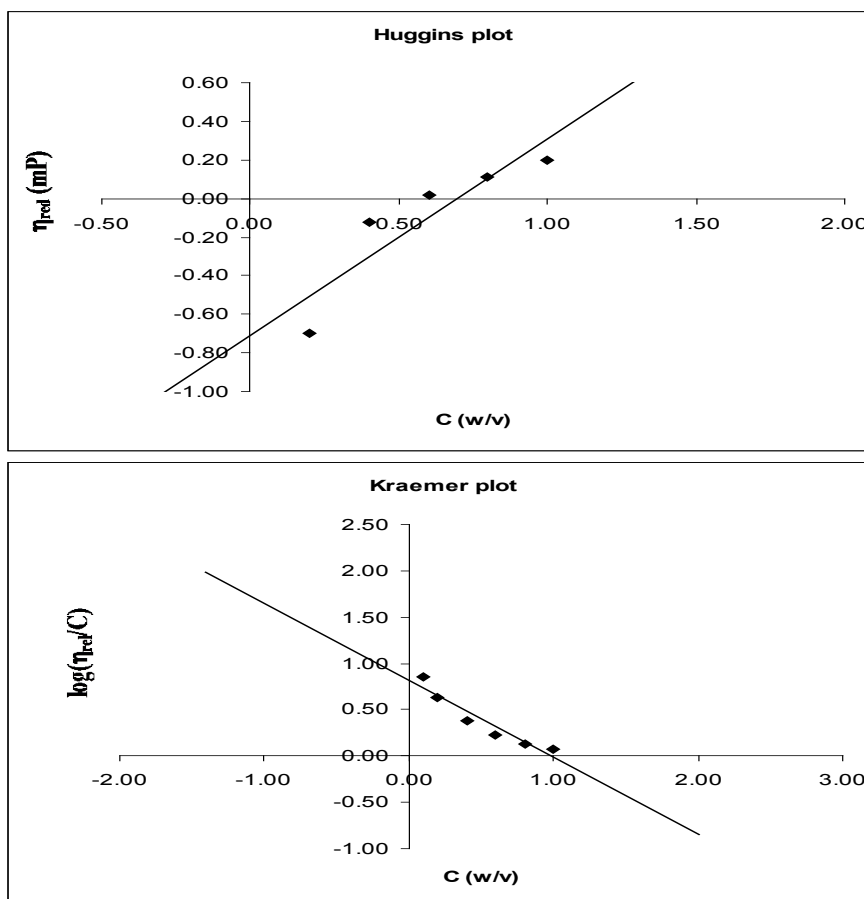


**Figure 8** Huggins and Kraemer plots for *Albizia zygia* gum.

Based on experimental observations, the physical meaning of the dimensionless Huggins coefficient  $k'$  can be summarized as follows: [17]

- a polymer exhibits a higher value of  $k'$  in a poor solvent than in a good solvent, i.e., when the polymer-polymer interactions become favorable over polymer-solvent interactions.
- it has a value of 0.5 - 0.7 in a theta solvent and (c)  $k'$  is very sensitive to the formation of molecular aggregates.

From the results obtained, values of  $[\eta]$  and  $k'$  approximates 0.8 and 0.6 respectively. This indicates that the degree of polymer-polymer interaction in *Albizia zygia* gum is relatively high. Higiroy *et al.* [6] also established that the intrinsic viscosity of a polymer can be calculated using the Kraemer equation, rather than the Huggins equation. Accordingly, the Kraemer equation can be written as follows:

$$\ln (\eta_{rel}/C) = [\eta] + k''[\eta]^2C \quad (7)$$

where  $k''$  is the Kraemer constant. From Eq. (7), a plot of  $\ln(\eta_{rel}/C)$  versus  $C$  should be a straight line with an intercept and slope equal to  $[\eta]$  and  $k''[\eta]^2$ , respectively. **Figure 8** also presents the Kraemer plots for *Albizia zygia* gum. Values of Kraemer parameters deduced from the plots are also recorded in **Table 4**. From the results obtained, calculated values of  $[\eta]$  and  $k''$  are comparable to those obtained from Huggins plots.

Huggins and Kraemer plots are centered on the extrapolation to zero concentration indicating that it is based on the calculation of intercepts. McMillan [18] found that methods of determination of the intrinsic viscosity that were based on slopes of plots have higher correlation coefficients and lower standard errors, compared with those based on intercepts of plots. On the bases of such findings, Tanglertpaibul and Rao [19] obtained 3 equations that can also be used in the determination of the intrinsic viscosity of a polymer. The equations are,

$$\eta_{rel} = 1 + [\eta]C \quad (8)$$

$$\eta_{rel} = \exp([\eta]C) \quad (9)$$

$$(1 - 1/\eta_{rel}) = [\eta]C \quad (10)$$

From Eq. (8),  $[\eta]$  is the slope obtained by plotting  $\eta_{rel}$  versus  $C$ . Also, the implication of Eq. (9) is that  $[\eta]$  is the slope obtained from the plot of  $\ln \eta_{rel}$  versus  $C$  and from Eq. (10),  $[\eta]$  is a slope obtained by plotting  $(1 - 1/\eta_{rel})$  versus  $C$ . Tanglertpaibul and Rao plots according to Eqs. (8), (9) and (10) for *Albizia zygia* gum are presented in **Figure 9**. Corresponding values of  $[\eta]$ ,  $R^2$  and intercepts deduced from the plots are presented in **Table 5**. The results revealed that the average value of the intrinsic viscosity is 0.5, compared to a value of 0.8 obtained from Huggins and Kraemer plots. Therefore, it can be assumed that the value of  $[\eta]$  for *Albizia zygia* gum lies between 0.5 and 0.8.

According to Higiro *et al.* [7], the power law equation relating specific viscosity and concentration can be expressed as follows:

$$\eta_{spec} = aC^b \quad (11)$$

If the logarithm of Eq. (11) is taken and rearranged, (12) is obtained

$$\log(\eta_{spec}) = \log(a) + b \log C \quad (12)$$

From Eq. (12), a plot of  $\ln(\eta_{spec})$  versus  $\log C$  should give a straight line with a slope and intercept equal to 'b' and 'loga' respectively.

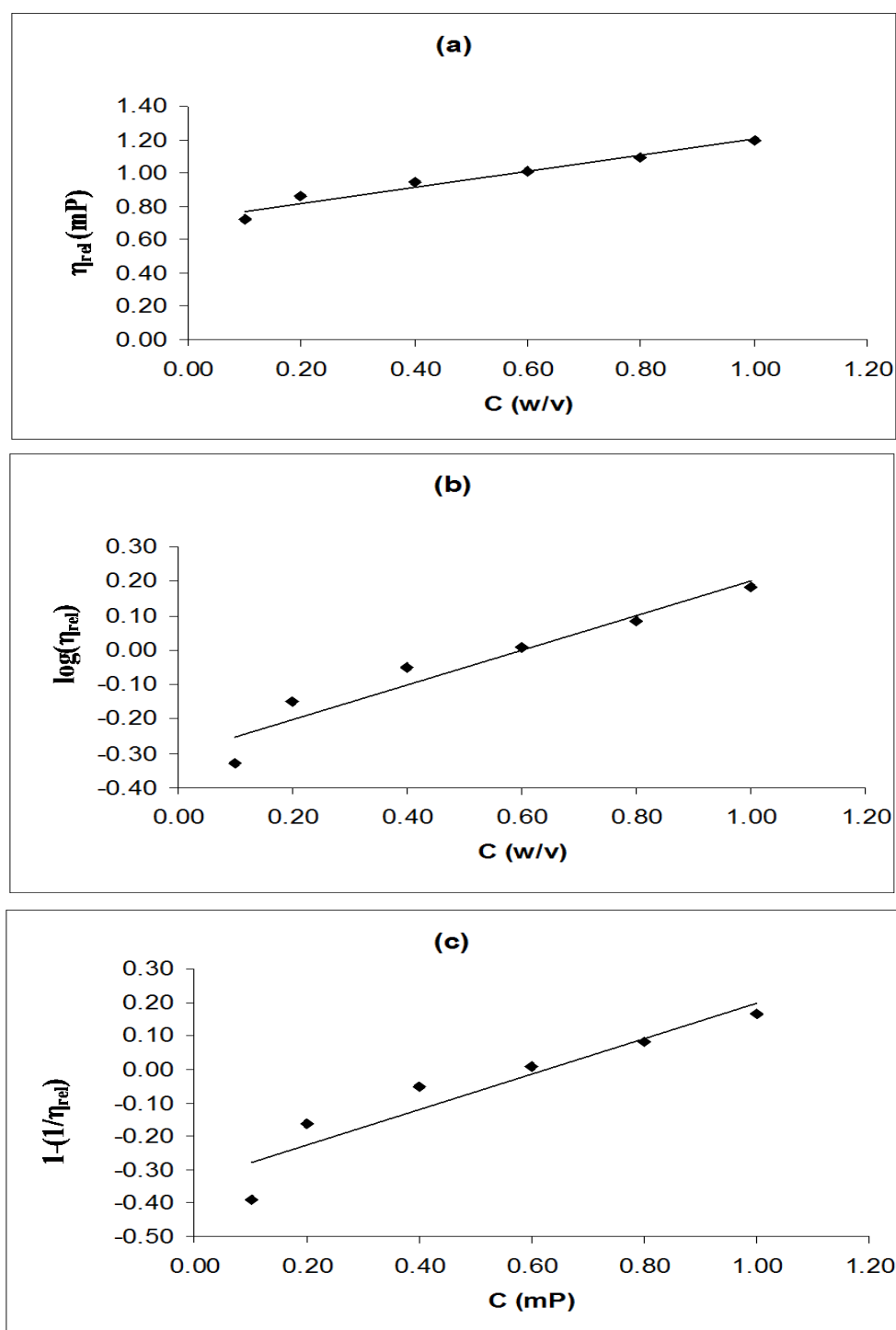


**Figure 9** Tanglertpaibul and Rao plots based on Eqs. (8), (9) and (10) for *Albizia zygia* gum.

**Table 5** Tanglertpaibul and Rao parameters for *Albizia zygia* gum.

|          | $[\eta]$ | Intercept | $R^2$  |
|----------|----------|-----------|--------|
| Eq 8 (a) | 0.4764   | 0.7255    | 0.9597 |
| Eq 9 (b) | 0.4998   | 0.3003    | 0.9293 |
| Eq 10(c) | 0.5334   | 0.3331    | 0.8861 |

**Figure 10** shows the power law plots for *Albizia zygia* gum. From the plot, calculated values of 'a'; and 'b' are 1.0654 and 0.2028, respectively. According to Lai *et al.* [20], the b value is an index that can be used to predict the conformation of a polymer. Also, Lapasin and Prici [21] stated that the b value greater than unity is associated with random coil conformation while the b value less than unity is associated with rod-like conformation. Therefore, molecular conformation

of *Albizia zygia* gum is less random coil-like than rod-like.

Based on the variation of shear rate with viscosity, colloidal systems such as gums can be classified as Newtonian or non-Newtonian. A Newtonian fluid is one in which the viscosity is independent of the shear rate. In Newtonian fluids, all the energy goes into sliding molecules by each other. In non-Newtonian fluids, the shear stress/strain rate relation is not linear and the viscosity typically drops at high shear rates.

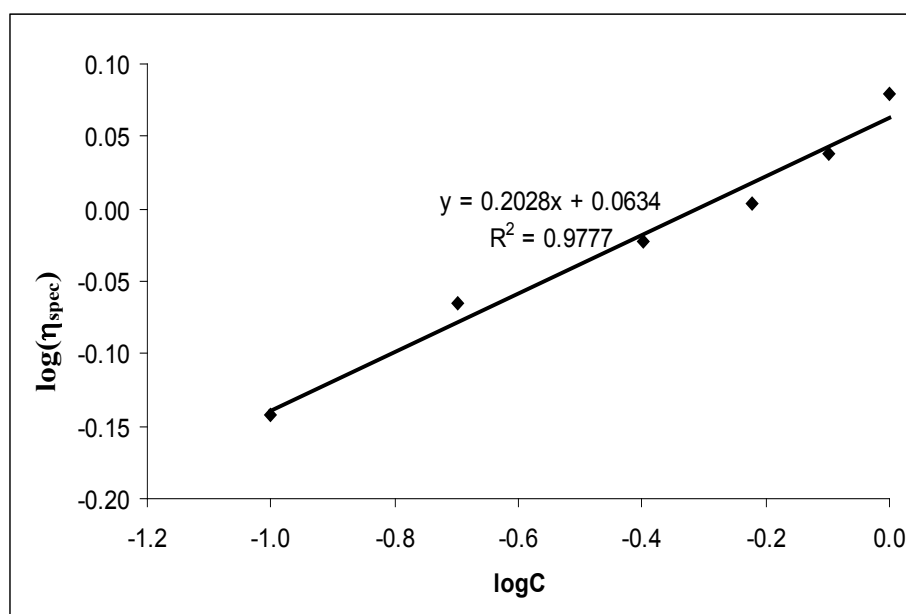


**Figure 10** Variation of  $\log(\eta_{\text{spec}})$  with  $\log C$  (power law plot) for *Albizia zygia* gum.

The behaviour of Newtonian colloids can be highlighted as follows;

- i. if the only stress generated in simple shear flow is the shear stress  $S$ , the two normal stress differences are zero;
- ii. the shear viscosity does not vary with shear rate;
- iii. the viscosity is constant with respect to the time of shearing and the stress in liquid falls to zero immediately after the shearing is stopped;
- iv. the viscosities measured in different types of deformation are always in simple proportion to one another.

Non-Newtonian fluids show deviation from the above listed features. The velocity gradient,  $dv/dx$ , is a measure of the speed at which the intermediate layers move with respect to each other. It describes the shearing the liquid experiences and is called shear rate ( $R$ ). The term  $F/A$  indicates the force per unit area required to produce the shearing action and it is called shear stress ( $S$ ). Therefore, viscosity can be defined as the ratio of shear stress to shear rate (i.e.: viscosity = shear stress  $S$ /shear rate  $R$ ). In order to determine Newtonian or non-Newtonian characteristics of gums, several methods have been reportedly used. However, one of the most commonly used methods for analyzing non-Newtonian flow involves the construction of a plot of viscosity versus spindle speed using the same spindle. If such plots are linear, then the fluid is said to be non-Newtonian. From the plot of speed of rotation versus viscosity (plot not shown), an  $R^2$  value of

0.8945 was obtained, indicating that *Albizia zygia* gum is a non Newtonian fluid. The relative yield value of the gum was also determined by extrapolating the line to zero rpm. The calculated yield value was found to be 145.38 mP. The power law index ( $N$ ) was determined using the following equation: power law index  $N = \tan$  (the angle between the plot line and y-axis). It has been found that if the angle is less than 45 degrees, the fluid is pseudoplastic, and if greater than 45 degrees, it is dilatant. The calculated angle for *Albizia zygia* gum was  $93.33^\circ$ , indicating that *Albizia zygia* gum is dilatant.

The power law index ( $N$ ) can also be used to calculate the effective shear rate at a given speed using the following equation,  $S = N/(0.2095 \times \text{viscometer speed in rpm})$ . **Figure 11** shows (a) the variation of viscosity with shear rate and (b) the variation of shear rate with shear stress for *Albizia zygia* gum. The Figures are typical for dilatant polymers. Therefore, *Albizia zygia* gum is a dilatant, with characteristic shear thickening property.

Our present results compare favorably with those reported by Mital *et al.* [22] and Mital and Adotey [23,24] for *Albizia zygia* gum. Therefore, *Albizia zygia* gum can be used for stabilization of emulsion [25]. The results also compare favourably with those reported by Mhinzi [3] and de Paul *et al.* [2] for some gums from the *Albizia* (Tanzania origin) and *Albizia lebbeks* species, respectively.

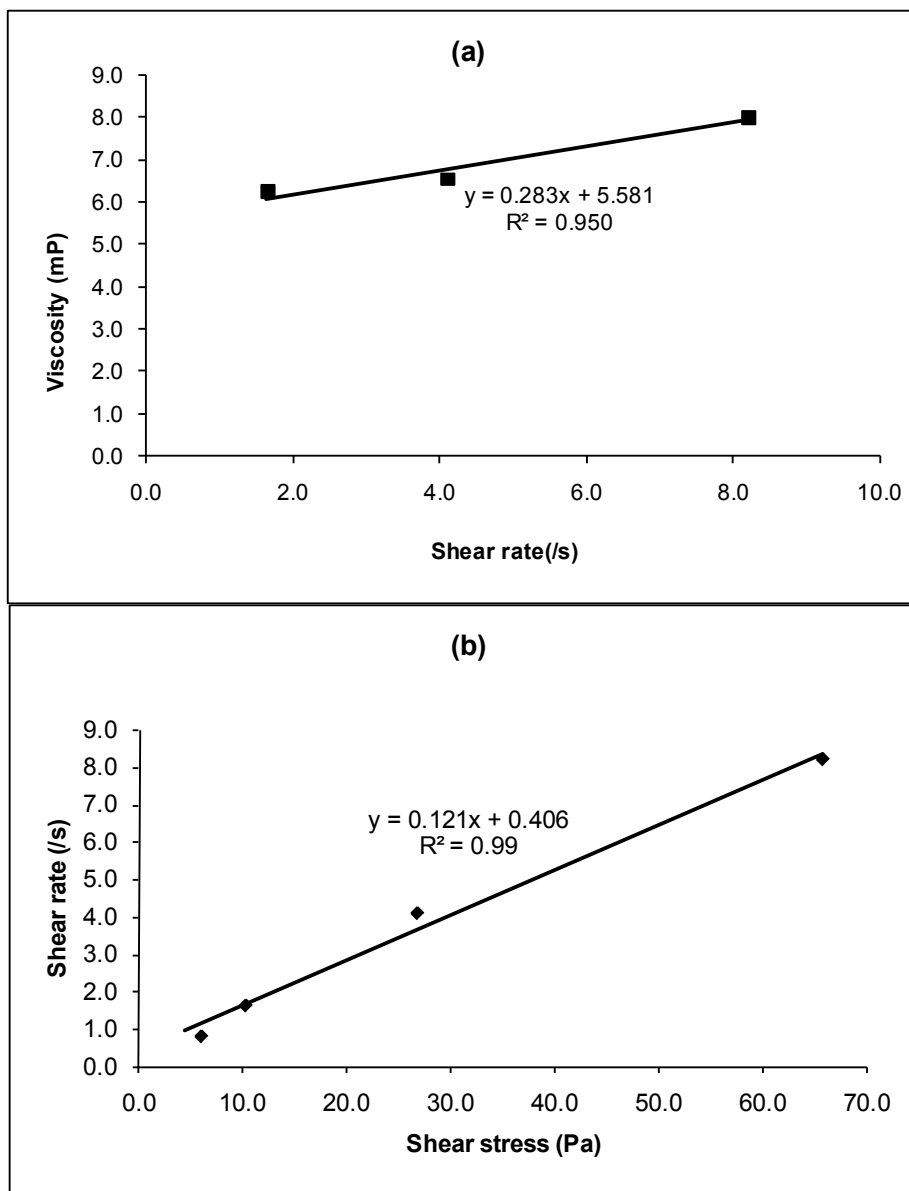


**Figure 11** Variation of (a) viscosity with shear rate and (b) shear rate with shear stress for *Albizia zygia* gum.

## Conclusions

From the results and findings of the study, the following conclusions are drawn,

i. *Albizia zygia* gum is dark brownish in colour, honey odour, bland tasting, acidic and ionic gum. The gum is soluble in cold and hot

water, sparingly soluble in ethanol, but insoluble in acetone and chloroform.

ii. The major chemical constituents of *Albizia zygia* gum include dimethyl phthalate, methyl palmitate, (9*E*,12*E*)-methyl octadeca-9,12-dienoate, (*E*)-methyl octadec-7-enoate, methyl stearate, 3-((aminomethoxy) (hydroxy)

phosphoryloxy)propane-1,2-diyl dipalmitate, methyl icosanoate, (Z)-octadec-13-enal, 2-hydroxy-3-(palmitoyloxy)propyl stearate, 2,3-dihydroxypropyl oleate and 2,3-dihydroxypropyl stearate. Chemical analysis of the gum reveals the absence of toxicant, indicating that the gum may have some food and pharmaceutical values.

iii The morphology of *Albizia zygia* gum reveals irregular shapes embedded within the surface, while its rheological properties indicated that the gum is non-Newtonian fluid and a dilatant with characteristic shear thickening property. These properties compare favourably with those of other gums used as binders for some drugs.

### Acknowledgement

The authors are grateful to Dr. Nnabuk Okon Eddy for sponsoring the research and to the Technical Staff of the Chemistry and Pharmacy Department, Ahmadu Bello University, for their support.

### References

- [1] SG Anema, KE Lowe and Y Li. Effect of pH on the viscosity of heated reconstituted skim milk. *Int. Dairy J.* 2004; **14**, 541-8.
- [2] RCM De Paul, SA Santana and JF Rodrigues. Composition and rheological properties of *Albizia lebbeck* gum exudate. *Carbohydr. Polymer.* 2001; **44**, 133-9.
- [3] GS Mhinzi. Properties of gum exudates from selected *Albizia* species from Tanzania. *Food Chem.* 2002; **77**, 301-4.
- [4] NE Siddig, ME Osman, S Al-Assaf, GO Phillips and PA Williams. Studies on acacia exudate gums, part IV. Distribution of molecular components in *Acacia seyal* in relation to *Acacia senegal*. *Food Hydrocolloids* 2005; **19**, 679-86.
- [5] HT Jalali, ZJ Ebrahimian, DV Evtuguin and CP Neto. Chemical composition of oleo-gum-resin *Ferula gummosa*. *Ind. Crop. Prod.* 2011; **33**, 549-53.
- [6] J Higiroy, TJ Herald and S Alavi. Rheological study of xanthan and locust bean gum in dilute solution. *Food Res. Int.* 2006; **39**, 165-75.
- [7] I Bonaduce, H Brecolaki, MP Colombini, A Liuveras, V Restivo and E Ribechini. Gas chromatographic-mass spectrometric characterization of plant gums in samples from painted works of art. *J. Chrom. A* 2007; **1175**, 275-82.
- [8] A Dutta and A Sarkar. FTIR investigation of structural change in bio-molecule. *Adv. Appl. Sci. Res.* 2011; **2**, 125-8.
- [9] J Zhang, S Xu, S Zhang and Z Du. Preparation and characterization of tamarind gum/sodium alginate composite gel beads. *Iranian Polymer J.* 2008; **17**, 899-906.
- [10] VF Monteiro, AM Natal, LEBSD Soledade and E Longo. Morphological analysis of polymers on hair fibers by SEM and AFM. *Mater. Res.* 2002; **3**, 501-6.
- [11] M Femi-Oyewo, O Musliu and O Taiwo. Evaluation of the suspending properties of *Albizia zygia* gum on sulphadimidine suspension. *Trop. J. Pharmaceut. Res.* 2004; **3**, 279-84.
- [12] SJ Carter. *Tutorial Pharmacy: Solution*. In: Great Britain, Pitman Press, 2005, p. 1-8.
- [13] X Ma and M Pawlik. Intrinsic viscosities and Huggins constants of guar gum in alkali metal chloride solutions. *Carbohydr. Polymer.* 2007; **70**, 15-24.
- [14] C Calvo, F Martinez-Checa, A Mota and E Quesada. Effect of cations, pH and sulfate content on the viscosity and emulsifying activity of the *Halomonas eurihalina* exopolysaccharide. *J. Ind. Microbiol. Biotechnol.* 1998; **20**, 205-9.
- [15] L Lar and HR Chiang. Rheology of decolorized hsian-tsao gum in the dilute domain. *Food Hydrocolloids* 2002; **16**, 427-40.
- [16] ML Huggins. The viscosity of dilute solutions of long-chain molecules. IV. Dependence on concentration. *J. Am. Chem. Soc.* 1942; **64**, 2716-8.
- [17] T Sakai. Huggins constant k' for flexible chain polymers. *J. Polymer Sci.* 1968; **6**, 1535-49.
- [18] DE McMillan. A comparison of five methods for obtaining the intrinsic viscosity of bovine serum albumin. *Biopolymers* 1974; **13**, 1367-71.
- [19] T Tanglertpaibul and MA Rao. Intrinsic viscosity of tomato serum as affected by methods of determination and methods of processing concentrates. *J. Food Sci.* 1987; **52**, 1642-88.

- [20] LS Lai, J Tung and PS Lin. Solution of hsian-tsao (*Mesona procumbens* Hemsl) leaf gum. *Food Hydrocolloids* 2000; **14**, 287-94.
- [21] R Lapasin and S Pricl. *Rheology of Polysaccharide Systems*. In: R Lapasin and S Pricl (eds.). *Rheology of industrial polysaccharides: Theory and applications*, Blackie Academic and Professional, Glasgow 1995; p. 250-494.
- [22] HC Mital, J Ocran and YD Fokuo. Studies on *Albizia* gum 4: Comparative assessment of rheological properties of *Albizia* and other mucilages. *Journal of Texture Studies* 1978; **9**, 325-34.
- [23] HC Mital and J Adotey. Studies of *Albizia zygia* gum; rheological properties of mucilages. *Pharm. Acta Helv.* 1972; **47**, 508-15.
- [24] HC Mital and J Adotey. Studies of *Albizia zygia* gum; certain physicochemical properties. *Pharm. Acta Helv.* 1971; **46**, 637-42.
- [25] HC Mital and J Adotey. Studies of *Albizia zygia* gum; Stabilizations of emulsions. *Pharm. Acta Helv.* 1973; **48**, 412-9.